Published in final edited form as:

Res Microbiol. 2017 September ; 168(7): 609–625. doi:10.1016/j.resmic.2017.04.005.

For publication Proteomic analysis of a mosquito host cell response to persistent *Wolbachia* infection

Gerald Baldridge[a], **LeeAnn Higgins**[b], **Bruce Witthuhn**[b], **Todd Markowski**[b], **Abigail Baldridge**[c], **Anibal Armien**[d], and **Ann Fallon**[a]

[a]Department of Entomology, University of Minnesota,1980 Folwell Ave., St. Paul, MN, USA 55108

[b]Department of Biochemistry, Molecular Biology and Biophysics, University of Minnesota, 6-155 Jackson Hall, 321 Church St. SE, Minneapolis, MN 55455

[c]Department of Preventive Medicine, Feinberg School of Medicine, Northwestern University, 680 N. Lake Shore Drive, Chicago, IL 60611

[d]Department of Veterinary Population Medicine, University of Minnesota, 1333 Gortner Ave., St. Paul, MN 55108

Abstract

Wolbachia pipientis, an obligate intracellular bacterium associated with arthropods and filarial worms, is a target for filarial disease treatment and provides a gene drive agent for insect vector population suppression/replacement. We compared proteomes of *Aedes albopictus* mosquito C/*w*Str1 cells persistently infected with *Wolbachia* strain *w*Str, relative to uninfected C7–10 control cells. Among approximately 2,500 proteins, iTRAQ data identified 815 differentially abundant proteins. As functional classes, energy and central intermediary metabolism proteins were elevated in infected cells, while suppressed proteins with roles in host DNA replication, transcription and translation suggested that *Wolbachia* suppresses pathways that support host cell growth and proliferation. Vacuolar ATPase subunits were strongly elevated, consistent with high densities of *Wolbachia* contained individually within vacuoles. Other differential level proteins had roles in ROS neutralization, protein modification/degradation and signaling, including hypothetical proteins whose functions in *Wolbachia* infection can potentially be manipulated by RNAi interference or transfection. Detection of flavivirus proteins supports further analysis of poorly understood, insect-specific flaviviruses and their potential interactions with *Wolbachia*, particularly in mosquitoes transinfected with *Wolbachia.* This study provides a framework for future attempts to manipulate pathways in insect cell lines that favor production of *Wolbachia* for eventual genetic manipulation, transformation and transinfection of vector species.

Correspondence and reprints: baldr001@umn.edu.

Conflict of interest

The authors have no conflicts of interest.

Keywords

Mosquito cell lines; *Aedes albopictus*; *Wolbachia pipientis*; intracellular bacterium; flavivirus; Transinfection

1. Introduction

The alphaproteobacterium, *Wolbachia pipientis* (*Rickettsiales; Anaplasmataceae*) is an obligate intracellular endosymbiont originally described in ovaries of *Culex pipiens* mosquitoes [1], and now known to be widely distributed among arthropods, including an estimated 40% of Culicine mosquitoes [2]. In mosquitoes, *Wolbachia* infection is associated with cytoplasmic incompatibility (CI), the reproductive distortion in which eggs of uninfected females fail to hatch if fertilized by sperm from an infected male [3, 4]. Because *Wolbachia* confers a reproductive advantage to infected females, the bacterium provides an attractive candidate for disease control through population suppression/eradication, first demonstrated nearly 50 years ago in Myanmar (Burma) with the filariasis vector, *Culex pipiens fatigans* [5, 6].

Interest in exploiting *Wolbachia* as a gene drive agent for control of vector-borne disease [4] has been stimulated by advances in genomics, including successful transformation of related intracellular bacteria [7]. In addition, *Wolbachia* reduces pathogen transmission following artificial introduction (transinfection) into mosquito species that do not harbor *Wolbachia* in nature, such as the *Aedes aegypti* vector of yellow fever, dengue, and Zika viruses and *Anopheles* vectors of human malaria [8, 9, 10, 11, 12]. Successful cage and field trials using Wolbachia-infected mosquitoes [13, 14, 15] strongly support intensified efforts to develop techniques for in vitro manipulation and genetic transformation of *Wolbachia* to facilitate its use as a biocontrol agent for vector-borne disease [2, 16, 17].

Cell lines that maintain high levels of *Wolbachia* provide a source of bacteria for genetic manipulation and subsequent recovery and amplification of transformants for introduction into target mosquitoes. Infected cell lines further provide an in vitro approach to investigating interactions with host cells, such as control of oxidative stress [18, 19], iron metabolism [20], chromatin remodeling [21, 22] and the molecular basis for CI [23]. The C/*w*Str1 cell line maintains a robust infection with the CI-inducing *Wolbachia* strain *w*Str [24, 25], which replicates in individual vacuoles surrounded by a host-derived membrane [26]. Among 790 *Wolbachia* proteins, we established a molecular ‘footprint’ of *w*Str infection dominated by chaperones, stress response and *Wolbachia* surface proteins [27].

Here we provide a quantitative proteomic analysis of the mosquito host cell response to *w*Str that suggests *Wolbachia* conforms to an emerging paradigm based on pathogenic intracellular bacteria in vertebrates that evade innate immunity responses and enhance access to host nutritional reserves [28, 29].

2. Materials and methods

2.1. Cultivation of cells, subcellular fractionation and preparation of protein extracts

Aedes albopictus C7–10 (control) and C/*w*Str1 (Wolbachia-infected) cells were maintained in Eagle's minimal medium supplemented with glucose, non-essential amino acids, glutamine, vitamins, penicillin/streptomycin and 5% fetal bovine serum at 28°C in a 5% CO_2 atmosphere as described previously [25, 27, 30]. For proteomic analysis, unsynchronized populations of exponentially growing cells from six 25-cm^2 flasks were recovered by gentle pipetting, followed by centrifugation of pooled cells to remove medium. Biological replicates included cells from passages (p) 9, 16 and 35; data from all samples were combined for the final analysis. Cells were washed with serum-free medium, and subcellular fractions were prepared by sonication, filtration, centrifugation and sucrose gradient fractionation as detailed previously [27] and summarized at left in Fig. 1.

2.2. Protein preparation

In an initial analysis of samples previously used to enumerate *Wolbachia* proteins (labeled D, E, F, G in Fig. 1; standard MS/MS shaded rectangle), *Aedes* host cell proteins were recovered from SDS PAGE gel lanes cut into 22 gel slices, subjected to in gel digestion with trypsin and analyzed by LC-MS/MS on an LTQ mass spectrometer (D and E). Samples F and G contained proteins recovered from the *Wolbachia*-enriched sucrose gradient fraction GF-50/60 that were digested in solution with trypsin for separation of peptides by reversed-phase high pressure liquid chromatography (HPLC) and identification on an Orbitrap mass spectrometer [27]. In a parallel quantitative analysis using the iTRAQ® peptide isobaric labeling technology and the Orbitrap Velos system, single samples of Wolbachia-infected C/*w*Str1 and uninfected C7–10 cell total cellular proteins (H in shaded ellipse, Fig. 1) and two samples each of cytoplasmic and mitochondrial proteins (I and J) were used for protein identification and quantitation.

The samples used for iTRAQ were prepared and labeled with isobaric tags at the Center for Mass Spectrometry and Proteomics at the University of Minnesota as described [31] with minor modifications. In brief, proteins were extracted with 8 M urea containing 0.2% SDS, 0.4 M triethylammonium bicarbonate pH 8.5 (TEAB) and 20% methanol, alkylated for 15 min at room temperature in 8 mM methyl methanesulfonate and digested with trypsin. The samples were cleaned, vacuum-dried and resuspended in 0.5 M TEAB, pH 8.5 to a final concentration of 2 μg/μl for labeling with isobaric tags (iTRAQ 4-plex reagent; AB Sciex, CA) and multiplexing. Data set H (see Fig. 1) was derived from 60 μg of C/*w*Str1 total cellular peptides labeled with isobaric tags 116 or 117 multiplexed with 60 μg C7–10 peptides labeled with tags 114 or 115. Data set I was derived from 19 μg of C/*w*Str1 peptides labeled with tags 115 (cyto) and 117 (mito) multiplexed with 19 μg C7–10 peptides labeled with tags 114 (cyto) and 116 (mito). Data set J was derived from a second preparation of C/*w*Str1 peptides labeled with tags 114 (cyto) and 116 (mito) multiplexed with C7–10 peptides labeled with tags 115 (cyto) and 117 (mito).

2.3. Mass spectrometry and protein identification

Tandem mass spectra were extracted by Sequest (Thermo Fisher Scientific, San Jose, CA, USA; version SRF v.3 or version 27, rev. 12) and searched against an rs_wolbachia_aedes_v200808_cRAP_flavivirusREV database that contained 74,570 protein entries from the *A. aegypti, Wolbachia* and flavivirus genomes as described previously [27]. We used the *A. aegypti* genome for validation of host proteins because the genomic data from the *A. albopictus* laboratory colony strain Foshan [32] was not yet available.

Scaffold (version 4.2.1, Proteome Software Inc., Portland, OR) was used to validate peptide detection and protein identifications from data sets D - G (Fig. 1). Peptide identifications were accepted at ≥ 95.0% probability by the Peptide Prophet algorithm [33]. Protein identifications assigned by the Protein Prophet algorithm [34] were accepted at ≥ 99% probability based on detection of at least two unique peptides. Sequest parameters, protein sequence database descriptions and program settings were detailed previously [27]. False discovery rates (FDRs) are reported in supplemental Table S1.

We searched the Orbitrap peptide tandem MS data sets (H, I and J; Fig. 1) from the iTRAQ® experiment with Protein Pilot 4.5 (Sciex, Foster City, CA) [35]. Search parameters included: cysteine MMTS; iTRAQ 4plex (Peptide Labeled); trypsin; instrument Orbi MS (1–3 ppm) Orbi MS/MS; biological modifications ID focus; thorough search effort; autobias correction; detected protein threshold > 0.05 (10%) and FDR analysis with reversed database. We applied a 1% global FDR to the protein summary report [36] and identified 2016 unique proteins, of which 815 had differential abundance in C/*w*Str1 relative to C7–10 protein extracts, and are reported in all tables as elevated (ratio > 1) or suppressed (ratio < 1).

Proteins were sorted into functional classes based on features such as NCBI website annotations, gene ontology, Keggs pathways and presence of conserved domains. Proteins with multiple activities/roles were subjectively assigned to a single functional class. Hypothetical proteins were classified as Function unknown unless protein sequence similarities or conserved domains revealed with Protein Cluster and BLASTp tools (http://BLAST.ncbi.nim.nih.gov) suggested alternate designations.

2.4. Statistical analysis

All tests of association were performed with SAS v9.4 (Cary, NC; http://www.sas.com/enus/home.html/). Details are described in legends to figures, tables and supplementary data.

2.5. Transmission electron microscopy

C/*w*Str1 cells were grown to near confluence in 25 cm^2 tissue culture flasks. The medium was carefully removed and cells were fixed overnight at 4°C in 2.5% glutaraldehyde in 0.1 M sodium cacodylate, pH 7.4. Cells were resuspended in fresh fixative, collected by centrifugation and post-fixed with 1% osmium tetroxide in 0.1 M sodium cacodylate buffer. The sample was dehydrated and embedded in Embed 812 resin, trimmed and sectioned; sections (60–70 nm) were contrasted with 5% uranyl acetate and Santos' lead citrate.

Sections were observed with a JEOL 1200 EX II transmission electron microscope (JEOL LTD, Tokyo, Japan).

3. Results

3.1. Overview

A. albopictus C/*w*Str1 cells infected with *Wolbachia* CI-inducing strain *w*Str from the planthopper, *Laodelphax striatellus* were grown in Eagle's medium supplemented with heat-inactivated fetal bovine serum. The robust infection (Fig. 2) was characterized by abundant cytoplasmic bacteria of variable morphology, enveloped individually within host cell membranes of unknown origin [26] as described previously for *Wolbachia* isolated from mosquito ovaries [1, 37]. For MS/MS analysis, proteins were recovered after cell fractionation and SDS-PAGE, and identities were assigned by searching a database that included host and *Wolbachia* proteins based on annotated genomes. In an initial analysis, we identified 790 *w*Str proteins and estimated their relative abundances using a statistical model of the relationship between protein mass and MS/MS-detected peptide count [27]. Here we report the host cell proteome of 2,471 proteins (hereafter referred to as *Aedes* proteins) from the same sample set supplemented by an additional quantitative iTRAQ analysis that identified a subset of 815 proteins with differential abundances in C/*w*Str1 cells relative to uninfected C7–10 cells. In the text below, we interpret the results in the context of potential molecular interactions between *w*Str and its host cells.

3.2. Derivation of an Aedes host cell proteome from C/wStr1 and uninfected C7–10 cells

We derived an *Aedes* host cell proteome using two data sets (Table 1). From sample sets D, E, F, and G, designated as the standard analysis in Fig. 1, we defined a *w*Str proteome of 790 proteins (italicized entries at right in Table 1) previously described in detail [27]. Here we focus on 9,848 identifications of peptides matched to host proteins which, after subtracting overlapping accessions, corresponded to 1,859 unique *Aedes* proteins. An additional iTRAQ analysis (data sets H, I and J in Fig. 1) recovered 3,177 protein identifications that corresponded to 2016 unique host proteins (Table 1). For consensus totals, proteins with ≥ 97% BLASTp sequence identity were assigned a single accession number. The Standard and iTRAQ data sets showed considerable overlap, with an aggregate total of 2,471 unique *Aedes* proteins identified with a confidence level of ≥ 99% from 13,025 identifications. The consensus proteins are reported in an EXCEL spreadsheet (Table S1, *Aedes* proteome sheet 1) by name, accession, molecular mass, identified peptide numbers, percent protein sequence coverage, protein functional class and comments. The *Aedes* proteome includes 560 hypothetical proteins, of which we assigned 300 to a functional class based on conserved domains and BLASTp analyses that suggested a cellular function.

3.3. *Validation of* Wolbachia *infection in iTRAQ samples*

In Table 1, data sets H, I and J from C/*w*Str1 cells were expected to contain *Wolbachia* proteins entirely absent from C7–10 cells, and thus excluded from iTRAQ-based quantification. Analysis of the peptide spectra identified 327 *w*Str proteins (Table S2, sheet 1), compared to 790 proteins previously described from the standard analysis [27]. A univariable statistical model of the relationship between protein mass and MS-detected

peptide count showed that log MW was a relatively weak (r-squared = 0.1394) but statistically significant (P < 0.0001) predictor of peptide count: log(peptides) = −0.23728 + 0.46866*log(mw). Based on that analysis, the majority of the 26 most abundant *w*Str proteins (Table S2, sheet 2) were from functional classes with the highest mean protein abundance levels (Suppl. Fig. S1).

3.4. Host proteins: Functional groups based on standard and iTRAQ data

Fig. 3 compares the functional class distribution of proteins from the standard (infected C/*w*Str1 cells, black bars; uninfected C710 cells, open bars) and iTRAQ (gray bars) samples normalized as fractional percentages of the largest class (protein modification/chaperones). In the standard analysis, differences in the number of proteins in C/*w*Str1 and C7–10 cells suggested that infected cells had a higher representation of proteins involved in energy, Transporters/Inorganic ion, lipid, secondary and amino acid metabolism (black diamonds in Fig. 3), compared to lower representation of proteins involved in motility/trafficking/secretion, Transcription/RNA modification, signal transduction, DNA replication/cell division, carbohydrate and nucleotide metabolism (white diamonds). With the exceptions of transcription and energy metabolism, distribution of proteins identified by iTRAQ approximated those of C/*w*Str1 values from the standard analysis (Fig. 3, compare black and gray columns).

Relative protein abundance based on ratios from isobaric tags differed for 815 proteins representing 33% of the 2,471 unique *Aedes* proteins. In Table S3, sheet 1, we provide the iTRAQ raw data for those 815 proteins. Where data were available from multiple samples, ratios were consistent among 305 proteins with elevated abundance in infected C/*w*Str1 cells and 495 with suppressed abundance. Although individual protein levels varied widely within each functional class, only 15 proteins had conflicting ratios in one or more extracts (Table S3, sheet 2).

Each iTRAQ ratio was log-transformed to support statistical analysis of differences in protein abundance by functional class. A univariable linear regression analysis of the mean log(ratio) of protein abundance, using protein functional class as a variable and the function unknown class as the referent, showed that differences between functional classes were statistically significant (F=15.84, P < 0.0001) with beta coefficients ranging from 0.54716 to −0.10658 (Table 2) correlating positively with mean log protein abundance (range: 0.23 to −0.42). Based on visual inspection of mean iTRAQ ratios on a linear scale (Fig. 4), we arbitrarily identified a cluster of six functional classes with average ratios ranging from 1.2 to 1.4-fold higher in C/*w*Str1 than control cells (Fig. 4; diamonds on or above line c), which suggested that *Wolbachia* infection was associated with increased energy, lipid, carbohydrate, amino acid, secondary and nucleotide metabolism. Five functional classes had average ratios from 1.0 to 1.2 (Fig. 4; diamonds between lines b and c), and included co-enzyme metabolism, motility/trafficking/secretion, general function, protein modification/chaperones and transporters/inorganic ion. The signal transduction and cytoskeleton/cell membrane classes were relatively unchanged. Five classes had ratios < 1 (Fig. 4; diamonds between lines a and b): cellular/pathogen defense, function unknown, transcription/RNA modification, ribosomes/translation and DNA replication/cell division. Based on these ratios,

the host response to C/*w*Str1 infection was characterized by higher abundance of proteins that support energy production and central intermediary metabolism, reduced abundance of proteins involved in DNA replication, transcription and translation, and relatively stable levels of proteins that participate in cellular maintenance.

3.5. Individual protein abundance levels and partitioning of metabolic resources

Table S4 summarizes Table S3, showing protein functional classes on individual sheets, and average iTRAQ ratios (calculated from Table S3, columns E, H, K, N and Q). Ratios > 0 indicate elevated abundance in infected C/*w*Str1 cells, while suppressed proteins have ratios < 0. In general, arithmetic averages giving equal weight to each of 815 proteins (Table 3) were in good agreement with the statistical analysis based on log-transformed values from 1307 observations (shown in parentheses in Table 3). Of the 815 proteins, 271 (33%) had ratios > 1.2, including individual proteins in all of the functional categories except DNA/cell division. Thirty-seven proteins (4.5%) had ratios ≥ 2, and these top-37 proteins were also distributed within several functional categories (Table 4). Below, we highlight some proteins, emphasizing those with increased abundance in infected cells, and focus the Discussion section on the top-37 proteins in the context of potential interactions and avenues for pharmacologic manipulation.

3.5.1. Energy metabolism—Over 7.5% of the differentially abundant proteins have roles in energy production (Table S4, sheet 1), of which 57%, including the glycolytic and most of the TCA cycle enzymes, were expressed at ratios exceeding the 1.2 threshold (Fig. 4). Ratios for key regulatory enzymes, phosphofructokinase (2.04) and pyruvate kinase (1.45) were elevated, as was lactate dehydrogenase (1.99), which interconverts lactate and pyruvate, with concomitant interconversion of NAD+ and NADH. Pyruvate dehydrogenase (1.67) converts pyruvate to acetyl-CoA, which enters the TCA cycle for further metabolism by citrate synthase (2.24) and malate dehydrogenase (1.31). Cytoplasmic malate dehydrogenase (2.65) is critical to the malate-aspartate shuttle, which regenerates NADH in the mitochondrial matrix, maximizing production of ATP from glucose.

3.5.2. Lipid metabolism—Of 39 proteins involved in lipid metabolism (Table S4, sheet 2), 74% had ratios > 1.2, and 10% were > 2.0, including 17 proteins (1.17 – 2.63) that participate in fatty acid metabolism in the cytoplasm, mitochondria or peroxisomes. These included two cytoplasmic acyl-CoA oxidases (1.43 and 1.56) as well as two mitochondrial acyl-CoA dehydrogenases (1.54 and 1.36) that initiate β-oxidation of fatty acids to provide reducing equivalents to the mitochondrial electron transport chain and acetyl-CoA to the TCA cycle. An elevated cytoplasmic glycerol-3-phosphate dehydrogenase (1.65) is a key enzymatic link between glycolysis and lipid metabolism which, in conjunction with the mitochondrial glycerol-3-phosphate dehydrogenase (1.55), functions in the glycerol phosphate shuttle, involved in regeneration of the cytosolic NAD^+ pool depleted by glycolysis. Sulfide quinone reductase (1.60) links sulfur amino acid and lipid metabolism/storage, while a sterol carrier protein (1.56) has a thiolase domain that influences intracellular lipid circulation. Six additional elevated proteins (1.11–1.85) have roles in transport of lipids and steroids that likely intersect with secondary metabolism of steroids.

3.5.3. Carbohydrate metabolism—Of 25 carbohydrate metabolism proteins (Table S4, sheet 3), several enzymes that participate in glycogen synthesis and degradation had increased ratios, suggesting that turnover of glycogen is an important feature of the *Wolbachia* infection. Key enzymes included the biosynthetic enzymes glycogen synthetase (1.74) and starch branching enzyme (1.69), and degradative enzymes glycogen phosphorylase (3.06) and phosphorylase b kinase (1.37). The ratio for glycogen phosphorylase is among the highest observed in this study, suggesting that generation of glucose, potentially as a precursor for increased synthesis of amino acids, supports *Wolbachia* maintenance and replication. Seven enzymes that function in the anabolic gluconeogenesis and pentose phosphate pathways that parallel glycolysis were elevated, including phosphoglucomutase (2.0) and 6-phosphogluconate dehydrogenase (1.86).

3.5.4. Amino acid metabolism—The *Aedes* proteome contained 51 proteins with primary roles in amino acid metabolism (Table S1, entries 2–52) of which 26 showed differential ratios in C/*w*Str1 cells (Table S4, sheet 4). Activities of glutamine (1.72) and asparagine (1.32) synthetases, glutamate dehydrogenase (1.66) and aspartate aminotransferases (1.55 and 1.72) link amino acid metabolism to the TCA cycle through α-ketoglutarate and oxaloacetate intermediates. Although glutamate cysteine ligase (1.23) was above 1.2, glutamate synthase (0.68) and cysteine desulfurylase (0.79), which have important roles in glutathione and sulfur metabolism, were among seven suppressed proteins (0.33–0.79). Upregulation of enzymes that generate glutamine and asparagine may compensate for depletion of host amino acid pools by *Wolbachia*, which lacks some amino acid biosynthetic pathways [38]. Glutamine is the most abundant amino acid in mammalian cells and is implicated in a number of signaling pathways, while the promoter for asparagine synthetase contains one of the better-known amino acid response elements [39, 40]. Although the mechanisms by which amino acid abundance regulates intracellular metabolism are poorly understood in mammalian cells, and have not been explored in insect cell lines, the likelihood that *Wolbachia* infection is associated with an overall deficiency in host amino acid pools is consistent with the general suppression of proteins that participate in transcription, translation and DNA replication.

3.5.5. Secondary metabolism—A strongly elevated farnesyl-pyrophosphate synthetase (1.95, Table S4, sheet 5) catalyzes an initial step in biosynthesis of squalene, dolichol, terpenes, steroids and juvenile hormone (JH), a terpene-based hormone unique to insects. An epoxide hydrolase (1.78) participates in regulating titers of JH by degrading it to an inactive diol. The *Aedes* homolog of estradiol 17-beta-dehydrogenase (2.02; 20-hydroxyecdysone dehydrogenase) converts ecdysone to a more active form, which in concert with JH regulates metabolism, growth and development in insects. Elevated cytochrome P450 enzymes (1.17 and 2.5) have insect homologs that are involved in steroid, terpenoid and xenobiotic metabolism. An elevated P450 homolog of Cyp304a1 (2.91) is involved in the stress response to DNA damage in *Drosophila.* Adrenodoxin, which functions as the mitochondrial P450 reductase, was suppressed (0.38). Enzymes with likely secondary functions in vitamin metabolism and lipid peroxidation included an aldehyde dehydrogenase (2.05), while an elevated leukotriene A-4 hydrolase (1.41) participates in metabolism of phopholipids,

arachidonic acid and eicosanoids in signaling pathways that affect kinases and other regulatory enzymes.

3.5.6. Nucleotide metabolism—Among 21 proteins, 13 had ratios above 1.2 (Table S4, sheet 6), including adenosine diphosphatase (2.07) and several nucleotide kinases that maintain nucleotide pools and influence activity of numerous enzymes as substrates or through regulatory interactions such as allosteric regulation of phosphofructokinase by ATP and AMP. Both subunits of ribonucleoside-diphosphate reductase required for synthesis of dNTP precursors were elevated (1.13 and 1.58). Adenylsulfate kinase (1.5) functions in the assimilation of sulfate and its incorporation into cysteine, methionine, glutathione, sulfolipids and iron-sulfur clusters, which are critical components of many proteins in energy production, electron transport, oxidative phosphorylation and other functions. Although most proteins with roles in purine and pyrimidine biosynthesis were suppressed, inosine-5-monophosphate dehydrogenase (1.26), which catalyzes the first step in guanine nucleotide synthesis and has regulatory effects in energy transfer, signal transduction and DNA/RNA synthesis, was elevated. The six suppressed enzymes (0.46 – 0.72) included adenylosuccinate synthetase, which catalyzes the first step in adenine nucleotide synthesis.

3.5.7. Co-enzyme metabolism—Nicotinate phophoribosyltransferase (1.34), which catalyzes the rate-limiting step in NAD salvage synthesis was elevated (Table S4, sheet 7), while hypothetical host protein AAEL002178 (0.83) and methylenetetrahydrofolate dehydrogenase (0.73), with roles in folate and glyoxylate metabolism, were among seven suppressed proteins (0.44–0.85).

3.5.7. Motility secretion and intracellular trafficking—Nine of 13 V-type H^+ ATPase subunits were elevated in the *Aedes* proteome (1.47–3.23; Table S4, sheet 8), including ATPase A (1.84) and the regulatory C (2.81) subunits of its V1 catalytic component. The V1 component hydrolyzes ATP, driving proton-pumping activity of the membrane-bound V0 assembly. Two isoforms of the V0 regulatory subunit were elevated (3.23 and 1.47) and potentially contribute to transport of nutrients into vacuoles occupied by *Wolbachia.* An elevated membrane traffic protein (1.86) contains an F-Bar dimerization module that influences membrane conformation. Among 23 proteins involved in ER/Golgi vesicle trafficking, only four were elevated (1.26–1.39), and 19 were suppressed proteins (0.31–0.78), including ERp44, a stress-induced ER protein that prevents secretion of proteins with unpaired cysteines and also modulates inositol triphosphate-dependent release of Ca^{2+}. Among 17 proteins involved in endosome, lysosome and autophagy processes, four were elevated, (1.2–2.08), including saposin (1.52), which facilitates lysosomal degradation of glycosphingolipds. The suppressed proteins included Atg3 (0.71) and Atg5 (0.72), which have roles in the maturation of autophagosomes in canonical autophagy. In contrast, non-canonical Atg-5 independent autophagy is critical in the life cycle of some intracellular microbes, such as *Francisella tularensis* replication, infection by *Brucella abortus*, and entry into vacuoles by *Mycobacterium marinum* [28]. Other autophagy-related proteins, including clathrin heavy chain (0.89) and five coated pit and vesicle formation proteins, two dynein (0.93, 0.87) and three myosin motor proteins (0.76, 0.69, 0.60) were suppressed, in contrast

to the elevated kinesin light (1.36) and heavy chain (1.24) subunits that carry cargo in anterograde transport to microtubule positive ends.

3.5.8. General function—Elevated general function proteins (Table S4, sheet 9) included a protein with a potential role in apoptosis (4.19), six hypothetical host proteins (1.28–2.61) with likely functions in metabolite processing and proteolysis, and bleomycin hydrolase (1.58), a cytoplasmic cysteine peptidase that forms a hexameric barrel ring reminiscent of the 26S proteasome cylindrical complex. A CRAL/TRIO domain protein with elevated levels (2.5) has general functions in lipophilic substrate transfer and in Ras/Rho GTPase family signaling pathways that regulate cell growth, cytoskeletal/membrane organization, motility and intracellular trafficking.

3.5.9. Protein modification, degradation and chaperones—Cytosolic chaperones, proteases and components of the 26S proteasome were generally elevated in C/*w*Str1 cells, consistent with a stress response accompanied by increased protein degradation (Table S4, sheet 10). Fourteen chaperones were elevated (1.14–1.68), including Hsp 10, 20, 60 and 90. Six proteases (1.15–1.85), including the major lysosomal protease, cathepsin D (1.58) were elevated, and twenty proteins (1.08–1.58) related to ubiquitin conjugation, activation, regulation and structure of the 26S proteasome complex were increased. Upregulation of proteasome subunits in newly-infected cells [41] suggests that *Wolbachia* may obtain amino acids from host proteasomal activity, as has been documented for *Legionella pneumophila* using a mutant that lacks the AnkB F-box effector protein [42]. Ratios for seven proteins that function in post-translational protein modification (1.21–1.72), including a UDP-glucosyltransferase (1.43) were increased, while suppressed proteins (0.46–0.88) primarily function in glycosylation, glycan formation and side chain modifications in the ER and Golgi. Calnexin (1.50) and calreticulin (1.31), which prevent maturation of mis-folded proteins in the ER, were elevated, but eight additional proteins with roles in protein folding and repair were suppressed (0.36–0.73).

3.5.10. Transporters and Inorganic ions—Differentially expressed proteins (Table S4, sheet 11) featured five hypothetical host proteins, of which two, AAEL010118 (3.66) and AAEL010816 (1.69), had strong BLASTp similarities to mitochondrial calcium uptake and phosphate carrier proteins. Transport proteins with increased ratios included a calcium-transporting ATPase (1.19), an inorganic pyrophosphatase (1.23), a mitochondrial phosphate carrier protein (1.37), and a mitochondrial solute carrier with ADP/ATP translocase activity (1.29). Suppressed proteins (0.42–0.75) included plasma membrane calcium (0.66) and sodium/potassium ATPases (0.67), a potassium/chloride symporter (0.60) from a family that transports amino acids and sugars, and an equilibrative nucleoside transporter (0.50), which transports nucleoside substrates into cells.

3.5.11. Signal transduction—Seven GTPase/GTP binding proteins were elevated (1.16–1.40, Table S4, sheet 12) and nine were suppressed (0.58–0.87), including hypothetical protein AAEL005197 (0.61) with domain and BLASTp identities to a RagA GTPase that activates mTORC1 associated with the vacuolar ATPase complex on the lysosomal surface in response to amino acid signaling. The mTORC1 complex also responds to membrane

receptor and phoshatidylinositol kinase signaling mediated by proteins such as an elevated inositol 1,4,5-triphosphate receptor (1.24), and hypothetical protein AAEL010678 (2.99), with a putative phopholipase C domain specific for phosphoinositides. Calcyphosine/tpp (1.34) participates in both phosphatidylinositol and cAMP-mediated signaling. One of two elevated cAMP-dependent kinase regulatory subunits (1.83) is a critical component of pathways that regulate glycogen, sugar and lipid metabolism that intersect with mTOR signaling. Protein phosphatase-2b, which functions as the catalytic subunit of calcineurin, a Ca^{2+}-calmodulin-dependent serine/threonine phosphatase that participates in signaling pathways, was elevated (1.38) and, in contrast to suppressed levels of phosphatase-1, (0.71) −2a (0.71) and −2c (0.82) with roles in regulation of glycogen metabolism, transcription and translation.

3.5.12. Cytoskeleton and cellular membranes—A strongly elevated annexin B9 (2.05; Table S4, sheet 13) is required for multivesicular body function and endosomal trafficking in *Drosophila*, and two annexin B10 proteins with actin-binding sites were also elevated (1.42 and 1.77). Annexins mediate Ca^{2+}-dependent membrane and protein interactions in endocytosis, signaling, motility and vesicle transport and lipid raft formation. Two flotillins (1.40, 1.54) and a hypothetical stomatin-like protein (AAEL004490; 1.42) with roles in lipid raft and caveolae formation were elevated. The *Aedes* proteome contains six actin isoforms (Table S1, entries 201–206), but none had ratios > 1.0. Coracle protein, which anchors other proteins to actin, was suppressed (0.62), as were 12 other proteins involved in actin filament formation, stabilization and membrane interactions (0.49 to 0.79; see the red entries in Table S4, sheet 13), while eight were elevated (range 1.0–1.45). Tubulin and putative microtubule-associated proteins were all suppressed, as were a cation-transporting ATPase (0.76) and a phospholipid scramblase (0.74), which influence membrane dynamics by mediating phospholipid transfer between leaflets.

3.5.13. Cellular and pathogen defense—Superoxide dismutases (1.84 and 1.88), glutathione peroxidases (2.10 and 1.51) and thioredoxin reductases (1.02 and 1.24), involved in neutralization of reactive oxygen species, were elevated, while catalase was suppressed (0.74.) Levels of peroxiredoxins (1.21, 0.74, 0.68, 0.46) involved in thiol-dependent ROS defense were mixed (Table S4, sheet 14).

3.5.14. Function unknown—Although only 12 of 61 proteins with unknown or putative functions had elevated levels in C/*w*Str1 protein extracts (Tables S4, sheet 15), they included the protein with the highest expression level, AAEL001471 (5.01), with a putative function in protein modification/degradation. Hypothetical protein AAEL004129 (0.56) has an ArfGap domain and sequence similarity to putative GTPase activating proteins for Arf, a regulator of mTORC1.

3.5.15. Transcription, translation and cell division—Proteins with the lowest iTRAQ ratios, representing processes that are suppressed in infected cells, included those involved in transcription (52 proteins; Table S4, sheet 16), translation (110 proteins; sheet 17) and DNA replication/cell division (44 proteins; sheet 18). Among proteins with roles in transcription and RNA modification, three were elevated, including a single DEAD box ATP-dependent

RNA helicase (1.79), which is a homolog of yeast *dbp*2, an enzyme that associates with chromatin, regulates fidelity of transcription initiation and influences ribonucleoprotein assembly by altering RNA structure. Seven additional DEAD box RNA helicases were among 49 suppressed proteins. The ribosomes/translation class included 110 proteins, of which six had elevated levels including serine (1.22), alanine (1.22) and glycine (1.18) tRNA synthetases. All cytosolic and mitochondrial ribosomal proteins were suppressed (0.45–0.86), as were ribosomal maturation and translation factors, and most tRNA synthetases and tRNA modification enzymes. Among 44 proteins with diverse roles in DNA replication, repair, packaging and cell division, all but a DNA topoisomerase (1.18) were suppressed. In aggregate, of 206 differentially expressed proteins with roles in DNA replication, cell division, transcription, RNA processing or translation, only 10 had increased levels in infected C/*w*Str1 cells.

3.6. Aedes hypothetical proteins

Of 560 hypothetical proteins in the *Aedes* proteome, 300 were assigned to a putative functional class. Of these, 75 are distributed throughout 17 of the 18 sheets showing iTRAQ ratios (Table S4, shaded as yellow entries). In addition, sheet 15 (function unknown) includes 52 hypothetical proteins among 61 entries. Thus, 136 (17%) of the 815 iTRAQ proteins are poorly known, of which 93% are hypothetical proteins. Table 5 highlights *Aedes* hypothetical proteins with C/*w*Str1 relative expression levels > 1.5 (shaded in gray; 9.4%) or < 0.5 (unshaded, 10.2%). Hypothetical protein AAEL001471 was strongly elevated (5.01) and contained zinc finger and UBA_SQSTM UBL domains found in ubiquitin-binding protein p62, a scaffolding protein that regulates endosomal signaling pathways and plays an important role in ubiquitin-mediated phagosomal clearance of intracellular *Listeria* and *Salmonella.* A potential role for this protein is consistent with known deficiencies in *Wolbachia*'s amino acid biosynthetic capacities and dependence on host amino acids. Likewise, a zinc-dependent peptidase (1.56) has potential function in provisioning *Wolbachia* with amino acids. Two phospholipases (2.99 and 1.86) also had high ratios, suggesting that degradation of host lipids also contributes to *Wolbachia*'s maintenance. Among the suppressed hypothetical proteins, three with potential roles in chromosome maintenance (0.48) and cell cycle regulation (0.40 and 0.35) were noteworthy in the context of an overall suppression of proteins that participate in DNA replication and cell division.

3.7. Flavivirus proteins

We detected unique peptides corresponding to flavivirus capsid, membrane and envelope structural proteins, as well as seven non-structural proteins from flaviviruses associated with mosquitoes and ticks. The majority of those peptides were present in total cellular and cytoplasmic extracts from both C/*w*Str1-infected and control cells subjected to gel fractionation to maximize protein detection (data sets D and E in Fig. 1), while the *Wolbachia*-enriched data sets F and G contained the fewest viral peptides. Table 6 summarizes the 95% confidence peptides matched to proteins from 10 better-known flaviviruses associated with hemorrhagic or encephalitic disease in humans, as well as flaviviruses unique to mosquitoes. Unique peptides ranged from three (1.6% coverage) for the insect-specific CFA described from an *Aedes aegypti* mosquito cell line [43], to 34

peptides that matched all WNV proteins except NS4A and NS4B, or 15.4% sequence coverage of the approximately 3400 amino acids within the viral polyprotein (Fig. S2).

4. Discussion

An important goal of our efforts to explore interactions between *Wolbachia* and insect cell lines that support its replication is development of protocols for mass production of this obligate intracellular bacterium, potentially manipulated by genetic technologies, for introduction into target insects. Although *Wolbachia* typically replicates in the reproductive tissues of its insect hosts [1, 6], successful transfer of *Wolbachia* strains between insect species [11] and into cultured cells [24, 25, 44, 45] indicates that *Wolbachia* do not require cell lines derived specifically from their host species or from reproductive tissues. For most insect cell lines, including C/*w*Str1, the tissue of origin is not known because tissue-specific markers are not available (reviewed in [46]). Because *Wolbachia* infects a wide range of insects and nematode worms, genetic manipulation will be facilitated by development of a "generic" host cell line that supports recovery and expansion of a wide range of *Wolbachia* strains. C/*w*Str1 mosquito cells maintain a persistent, high-density infection with *Wolbachia* strain *w*Str from the planthopper *Laodelphax striatellus* [24]. In these cells, individual bacteria are enveloped by a single host-derived membrane, as was described in pioneering observations with mosquito ovaries [1, 37, 47].

As an obligate intracellular bacterium, *Wolbachia* has a streamlined genome and reduced metabolic capabilities [38], making its growth and replication dependent on host cell precursors or products derived from breakdown of complex host cell macromolecules such as glycogen, lipids, and proteins. Evidence for competition between *Wolbachia* and host cells in culture includes a twofold increase in cell density when infected cells are plated in medium containing tetracycline/rifampicin, which suppress *Wolbachia* [25]. Infection of naive cells with *Wolbachia* is accompanied by increased ubiquitylation, suggesting use of proteasome-generated precursors [41]. A decrease in *Wolbachia* levels when culture medium is depleted of riboflavin suggests dependence on metabolically healthy host cells, as *Wolbachia* itself retains a metabolic capacity for riboflavin synthesis [48]. Differential responses to paraquat suggest that, relative to its host cell, *Wolbachia* is more sensitive to oxidative damage [49].

The present proteomic comparison of *w*Str infected and uninfected *A. albopictus* mosquito cells provides one of the first systematic investigations of a host cell response to *Wolbachia* infection. Among 2,471 unique proteins grouped according to functional class, a standard MS/MS analysis based on differences in number of protein identifications was in good agreement with quantitative iTRAQ data based on ratios of isobaric tags. To date, these data provide the most comprehensive proteomic analysis with mosquitoes (reviewed in [50]). For the majority of the 815 proteins detected by iTRAQ, increases or decreases in relative levels were within 2-fold, suggesting that C/*w*Str1 cells maintain homeostasis within a relatively narrow range of protein expression, providing sufficient amino acid and lipid resources for maintenance of a persistent *Wolbachia* infection despite suppression of host cell transcription, translation and cell division.

Aside from exploring overall metabolic change that accompanies a persistent *w*Str infection, we sought to identify potential targets that could be manipulated to provide a selective advantage to the infected cell. We envision use of genetic technologies to develop a cell line that exhibits improved growth after *Wolbachia* infection. Conditions under which *Wolbachia* provides positive selection would enhance efforts to develop efficient transformation procedures and allow recovery of genetically manipulated strains. Towards that end, we focus the following discussion on the 4.7% of proteins (Table 4; top-37 proteins) for which increased expression in infected cells exceeded a threshold ratio of 2.0, emphasizing pathways susceptible to pharmacological and/or genetic manipulation in host cells.

Neurotactin, a cell surface glycoprotein expressed during *Drosophila* development, had the highest ratio (5.33) for differential expression in *Wolbachia*-infected cells. In embryos of *Drosophila*, neurotactin occurs at sites of cell-cell contact, with eventual localization to nervous or endocrine systems. The protein contains an extracellular domain with homology to serine esterases, but lacks the active site and is highly susceptible to proteolytic degradation [51]. Although it is tempting to speculate that antisense expression of neurotactin might reduce the strongly adhesive properties of *w*AlbB-infected Aa23 cells [52], we note that, in a converse experiment with non-adhesive *Drosophila* S2 cells, transfection with the neurotactin gene did not increase cell-cell interaction [53].

Six top-37 proteins (Table 4) were hypothetical proteins, including AAEL001471, the second most highly elevated protein (5.01), which has domains suggestive of a role in ubiquitin-mediated proteolysis that would provide amino acids to *Wolbachia.* Many ubiquitin-related proteins were moderately elevated in infected cells. AAEL008862 (1.56) may encode a zinc-dependent peptidase. Two suppressed proteins AAEL011155 (0.40) and AAEL008569 (0.39) have motifs associated with cyclins, consistent with reduced expression of proteins involved in DNA replication and cell division (Table 5).

We speculate that hypothetical proteins associated with *Wolbachia* infection may be poorly known, in part because mosquitoes, unlike fleas and ticks, do not transmit bacterial pathogens. Mosquito cells respond to heat-killed extracellular bacteria by induction of various defensive proteins, including cecropins, defensins, transferrin and lysozyme [54], none of which are highly expressed in Wolbachia-infected cells. Deficiencies in the *Wolbachia* cell wall [38] may allow *Wolbachia* to avoid a typical immune response; alternatively, *Wolbachia* may secrete as yet unidentified effector proteins with protective functions. Elucidating functions of hypothetical proteins remains a key problem in molecular biology, exemplified by the recent finding that, of 473 genes comprising the genome of synthetic microbe Syn 3.0, 149 have unknown functions [55].

Subunits of the vacuolar, or V-type, H+ATPase complex account for 5 of the top-37 entries and constitute an obvious group of upregulated host proteins with a common function. V-ATPase shares a common ancestor with the F-ATPases of eubacteria, mitochondria and chloroplasts. In a previous study [27], we detected 7 subunits of the *Wolbachia* F_0F_1 ATPase, of which two were here among the most abundant *w*Str proteins (Table S2, sheet 2). We note that the F-ATPases produce ATP, while the V-ATPases utilize ATP.

V-ATPase is comprised of 14 subunits that form a cytosolic V1 complex associated with ATP hydrolysis, and a membrane-embedded V0 complex, which transports H^+ into vesicles or into the extracellular fluid. Acidification of intracellular compartments contributes to a wide range of intracellular functions, including dissociation of ligands from receptors, proteolytic processing of peptides such as insulin, and degradation of macromolecules by acidic hydrolases, including proteases, nucleases, glycosidases and lipases. Dissociation of the V1 and V0 complexes occurs in response to glucose deprivation; reassembly is mediated by the glycolytic enzyme aldolase, functioning as a glucose sensor [56].

By convention, the soluble V1 subunits and membrane-associated V0 subunits of V-ATPase are distinguished by capital and lower-case letters, respectively. The 116 kDa V0 subunit i was most highly expressed (3.23), and V1 subunits C (2.81), D (2.73), E (2.20) and H (2.75) were also highly elevated in infected cells. It will be of particular interest to learn whether a *Wolbachia*-encoded effector molecule modulates expression of host-encoded V-ATPase components, which potentially facilitate transfer of nutrients from host cytoplasm to the bacterium. We note that RNAi-mediated reduction of vATPase subunit transcripts severely inhibited mTORC1 signaling in cultured *Drosophila* S2 cells [57].

The malaria parasite, *Plasmodium falciparum* exports a functional V-ATPase into the erythrocyte host cell, where it targets the plasma membrane and plays a role in maintenance of intracellular pH [58]. Suppression of V-ATPase with bafilomycin reduces dengue infection in adult mosquitoes [59] and in mosquito cell lines [60], presumably because acidification of the endosome is required for release of virions into the cytoplasm. Inhibitors of V-ATPases, such as bafilomycin and concanamycin, and of F-ATPases, such as oligomycin [61], provide potential tools for investigating V- and F-ATPases in establishment and maintenance of *Wolbachia* infection.

Finally, V-ATPase has been implicated in an amino acid signaling pathway that regulates autophagy [62]. Autophagy is constitutively involved in cellular homeostasis, and the best-studied “canonical” autophagy responds to AMP-activated protein kinase and mTOR inhibition. Formation of non-canonical pathogen-specific autophagosomes, or xenophagy, is initiated through different pathways, and recruits proteins that do not participate in the canonical pathway. Intracellular microbes including *Anaplasma, Coxiella, Franciscella, Legionella, Mycobacterium*, and *Salmonella* evade xenophagy while stimulating canonical autophagic processes that increase intracellular nutrient pools from which they benefit [28]. *Anaplasma phagocytophilum*, which like *Wolbachia* is classified in the Anaplasmataceae, modulates mitochondrial function and apoptosis through the secreted T4SS effector, Ats1. Ats1 shuttles between mitochondria and autophagosomes, delays apoptosis by inhibiting release of cytochrome *c* from mitochondria and may also have a role in autophagosome inititation [29].

One additional protein in the motility/trafficking/secretion class is the Zeta-coat protein, which resembles clathrin in formation of vesicles that transport molecules within cells. Recent evidence suggests that, in a green alga, formation of these vesicles may be reduced by treatment with the phosphatidylinositol kinase inhibitor, wortmannin [63]. We note, however, that application of wortmannin to C/*w*Str1 cells can be complicated by its short

half-life in culture media (8–13 minutes), and off-target effects such as induction of nitric oxide production and protein phosphorylation (http://www.enzolifesciences.com/BML-ST415/wortmannin/).

A suite of six potentially related proteins is involved in carbohydrate metabolism. Activated by phosphorylase kinase (2.12), glycogen phosphorylase (3.06) is the rate-limiting enzyme in the conversion of glycogen to glucose 1-phosphate, which is converted to glucose 6-phosphate by phosphoglucomutase (2.00). Depending on the energy requirements of the cell, glucose 6-phosphate enters the glycolytic pathway to produce ATP, or the pentose phosphate pathway to produce ribose/NADPH. Phosphofructokinase (2.04) is the key regulatory enzyme in the glycolytic pathway, suggesting a glycolytic fate for glucose 6-phosphate. High expression of citrate synthase (2.24) provides support for upregulation of the TCA cycle, and phosphoenolpyruvate carboxykinase (2.48), which catalyzes the commitment step in gluconeogenesis, acts at the junction between the TCA cycle and glycolysis. Malate dehydrogenase (2.65) participates in the TCA cycle and in gluconeogenesis. Increased expression of pathways involved in carbohydrate metabolism may supplement pools of amino acids that cannot be synthesized by *Wolbachia*, as well as precursors for nucleic acid and lipid biosynthesis. The potential role of glycogen metabolism in cancer progression has stimulated interest in drugs such as 2-deoxyglucose and 1,4-dideoxy-1,4-amino-D-arabinitol, which target enzymes in glycogen metabolism [64].

Among the top 37 proteins, participants in oxidation-reduction reactions included six dehydrogenases (2.02–2.65), a cytochrome oxidase subunit (2.43), and glutathione peroxidase (2.1). The elevated levels of superoxide dismutases, peroxidases and thioredoxins indicated an oxidative stress response in infected cells, potentially associated with a cellular mechanism for *Wolbachia* suppression [18]. Studies with paraquat indicate that *Wolbachia* are more sensitive to oxidative damage than host cells [46], and an Ahp/Tsa antioxidant is among the most abundant *w*Str proteins (Table S2, sheet 2 and [27]). However, antioxidant gene expression and ROS levels did not vary significantly in tetracycline-cured Aa23 cells infected with *w*AlbB, *w*Mel or *w*MelPop strains [65]. Other top-37 proteins included two 3-hydroxyacyl-CoA dehydrogenases (2.63, 2.52) and short chain dehydrogenase (2.04) involved in fatty acid metabolism, an aldehyde dehydrogenase (2.05) that may participate in detoxification, and a mosquito homolog of the estradiol 17 beta-dehydrogenase, which likely plays a role in metabolism of the insect steroid hormone 20-hydroxyecdysone, an inhibitor of the cell cycle in mosquito cells [66].

Although not among the top-37 proteins, we identified peptides from flaviviruses in both infected and uninfected *A. albopictus* cells. Over 70 flaviviruses representing nine serogroups have been described, including dual-host flaviviruses such as Yellow fever, Zika, Chikungunya and West Nile that are important pathogens in humans [67]. Insect-specific flaviviruses that do not infect vertebrates have been isolated from mosquitoes worldwide, and flavivirus-like sequences, including some that encode open reading frames, are integrated into mosquito genomes (reviewed in [43]). Although potential interaction between *Wolbachia* and endogenous viruses remains unexplored, we note that West Nile virus can be transmitted transovarially from female to offspring [68, 69], suggesting that in *Wolbachia* infected-mosquitoes, virus and bacterium co-occupy the ovarian niche. Cell fusion agent,

discovered over 40 years ago in an *A. aegypti* cell line [70], occurs widely in field-caught and laboratory strains of *A. aegypti* [43], a species into which *Wolbachia* has been introduced by transinfection [11]. Mechanisms by which *Wolbachia* inhibits pathogen infections in transinfected mosquitoes can be variable and are not well understood [12, 71]. Likewise, superinfection exclusion (homologous interference) between mosquito-specific and dual host flaviviruses in cell lines is variable [43], suggesting a need for systematic investigation of potential interaction between endogenous flaviviruses and the better-known human pathogens in the mosquito host.

In aggregate, proteomic evidence for altered autophagy, metabolic signaling and protein degradation pathways, coupled with elevated vATPase, amino acid metabolism and TCA cycle proteins suggested that *w*Str's replication within host derived vacuoles evades xenophagy and sequesters host-derived amino acids. Elevated levels of proteases support earlier evidence for enhanced proteasome activity in *A. albopictus* cells infected with *w*AlbB [41] and potentially increase access to host amino acid pools. An integrated metabolomic, transcriptomic and proteomic analysis of the tick ISE6 cell line infected with *Wolbachiäs* relative, *A. phagocytophilum*, likewise suggests that infection is accompanied by changes in glucose metabolism, protein processing, and manipulation of autophagy [72]. A wide array of altered-level chaperones and protein folding, modification and trafficking proteins suggests a similar dynamic in C/*w*Str1 cells. *Wolbachia*-infected cells provide direct evidence for differential expression of several hypothetical *Aedes* proteins and a potential system for investigating their functions. Finally, we have identified targets that could be explored by RNAi knockdown of gene expression or in genetically manipulated cell lines. In future experiments, it will be of particular interest to explore effects of available pharmaceutical agents on *Wolbachia* growth kinetics, abundance and ability to infect cell lines, and to compare expression of proteins in cell lines to that of infected tissues in the insect host.

Supplementary Material

Refer to Web version on PubMed Central for supplementary material.

Acknowledgments

This work was supported by grant 5 R01 AI 081322 from the National Institutes of Health and by the University of Minnesota Agricultural Experiment Station, St. Paul, MN.

References

1. Hertig M. The rickettsia, *Wolbachia pipientis* (gen. et sp.n) and associated inclusions of the mosquito. Culexpipiens Parasitology. 1936; 38:453–486.
2. Bourtzis K, Dobson SL, Xi Z, Rasgon JL, Calvitti M, Moreira LA, et al. Harnessing mosquito-*Wolbachia* symbiosis for vector and disease control. Acta Trop. 2014; 132:S150–63. DOI: 10.1016/j.actatropica.2013.11.004 [PubMed: 24252486]
3. Bourtzis, K., Braig, HR., Karr, TL. Cytoplasmic incompatibility. In: Bourtzis, K., Miller, T., editors. Insect Symbiosis. Vol. 1. CRC Press; New York: 2003. p. 217-246.
4. Sinkins SP, Gould F. Gene drive systems for insect disease vectors. Nat Rev Genet. 2006; 7:427–435. [PubMed: 16682981]

5. Laven H. Eradication of *Culex pipiens fatigans* through cytoplasmic incompatibility. Nature. 1967; 216:383–384. [PubMed: 4228275]
6. Yen JH, Barr AR. New hypothesis of the cause of cytoplasmic incompatibility in *Culex pipiens* L. Nature. 1971; 232:657–658. [PubMed: 4937405]
7. Beare PA, Sandoz KM, Omsland A, Rockey DD, Henzein RA. Advances in genetic manipulation of obligate intracellular bacterial pathogens. Front Microbiol. 2011; 2:97.doi: 10.3389/fmicb.2011.00097 [PubMed: 21833334]
8. Kambris Z, Cook PE, Phuc HK, Sinkins SP. Immune activation by life-shortening *Wolbachia* and reduced filarial competence in mosquitoes. Science. 2009; 326:134–6. DOI: 10.1126/science.1177531 [PubMed: 19797660]
9. Yeap HL, Mee P, Walker T, Weeks AR, O'Neill SL, Johnson P, et al. Dynamics of the "popcorn" *Wolbachia* infection in outbred *Aedes aegypti* informs prospects for mosquito vector control. Genetics. 2011; 187:83–95.
10. Bian G, Joshi D, Dong Y, Lu P, Zhou G, Pan X, et al. *Wolbachia* invades *Anopheles stephensi* populations and induces refractoriness to *Plasmodium* infection. Science. 2013; 340:748–751. [PubMed: 23661760]
11. Hughes GL, Rasgon JL. Transinfection: a method to investigate *Wolbachia*-host interactions and control arthropod-borne disease. Insect Mol Biol. 2014; 23:141–151. [PubMed: 24329998]
12. Johnson KN. The impact of *Wolbachia* on virus infection in mosquitoes. Viruses. 2015; 7:5705–5715. DOI: 10.3390/v7112903 [PubMed: 26556361]
13. Walker T, Johnson PH, Moreira LA, Iturbe-Ormaetxe I, Frentiu FD, McMeniman CJ, et al. The *w*Mel *Wolbachia* strain blocks dengue and invades caged *Aedes aegypti* populations. Nature. 2011; 476:450–453. [PubMed: 21866159]
14. Hoffmann AA, Montgomery BL, Popovici J, Iturbe-Ormaetxe I, Johnson PH, Muzzi F, et al. Successful establishment of *Wolbachia* in *Aedes* populations to suppress dengue transmission. Nature. 2011; 476:454–57. [PubMed: 21866160]
15. O'Connor L, Plichart C, Sang AC, Breisforad CL, Bossin HC, Dobson SL. Open release of male mosquitoes infected with a *Wolbachia* biopesticide: field performance and infection containment. PLoS Negl Trop Dis. 2012; 6:e1797.doi: 10.1371/journal.pntd.0001797 [PubMed: 23166845]
16. Ricci I, Valzano M, Ulisse U, Epis S, Cappelli A, Favia G. Symbiotic control of mosquito borne disease. Pathog Glob Health. 2012; 106:380–85. DOI: 10.1179/2047773212Y.0000000051 [PubMed: 23265608]
17. LePage D, Bordenstein SR. *Wolbachia*: Can we save lives with a great pandemic? Trends Parasitol. 2013; 29:385–393. DOI: 10.1016/j.pt.2013.06.003 [PubMed: 23845310]
18. Brennan LJ, Keddie BA, Braig HR, Harris HL. The endosymbiont *Wolbachia pipientis* induces the expression of host antioxidant proteins in an *Aedes albopictus* cell line. PLoS ONE. 2008; 3:e2083.doi: 10.1371/journal.pone.0002083 [PubMed: 18461124]
19. Zug R, Hammerstein P. *Wolbachia* and the insect immune system: what reactive oxygen species can tell us about the mechanisms of *Wolbachia*-host interactions. Front Microbiol. 2015; 6:1201.doi: 10.3389/fmicb.2015.01201 [PubMed: 26579107]
20. Gill AC, Darby AC, Makepeace BL. Iron necessity: the secret of *Wolbachiäs* success? PloS Negl Trop Dis. 2014; 8:e3224.doi: 10.1371/journal.pntd.0003224 [PubMed: 25329055]
21. Riparbelli MG, Giordano R, Ueyama M, Callaini G. *Wolbachia*-mediated male killing is associated with defective chromatin remodeling. PloS One. 2012; 7:e30045.doi: 10.1371/journal.pone.0030045 [PubMed: 22291901]
22. Yuan LL, Chen X, Zong Q, Zhao T, Wang JL, Zheng Y, et al. Quantitative proteomic analyses of molecular mechanisms associated with cytoplasmic incompatibility in *Drosophila melanogaster* induced by *Wolbachia*. J Proteome Res. 2015; 14:3835–47. DOI: 10.1021/acs.jproteome.5b00191 [PubMed: 26220534]
23. Beckmann JF, Fallon AM. Detection of the *Wolbachia* protein WPIP0282 in mosquito spermathecae: implications for cytoplasmic incompatibility. Insect Biochem Mol Biol. 2013; 43:867–78. DOI: 10.1016/j.ibmb.2013.07.002 [PubMed: 23856508]
24. Noda H, Miyoshi T, Koizumi Y. *In vitro* cultivation of *Wolbachia* in insect and mammalian cell lines. In Vitro Cell Dev Biol Anim. 2002; 38:423–427. [PubMed: 12534342]

25. Fallon AM, Baldridge GD, Higgins LA, Witthuhn BA. *Wolbachia* from the planthopper *Laodelphax striatellus* establishes a robust, persistent, streptomycin-resistant infection in clonal mosquito cells. In Vitro Cell Dev Biol Anim. 2013; 49:66–73. DOI: 10.1007/s11626-012-9571-3 [PubMed: 23271364]
26. Serbus LR, Casper-Lindley C, Landmann F, Sullivan W. The genetics and cell biology of Wolbachia-host interactions. Annu Rev Genet. 2008; 42:683–707. DOI: 10.1146/annurev.genet.110306.130354 [PubMed: 18713031]
27. Baldridge GD, Baldridge AS, Witthuhn BA, Higgins LA, Markowski TW, Fallon AM. Proteomic profiling of a robust *Wolbachia* infection in an *Aedes albopictus* mosquito cell line. Mol Microbiol. 2014; 94:537–56. DOI: 10.1111/mmi.12768 [PubMed: 25155417]
28. Steele S, Brunton J, Kawula T. The role of autophagy in intracellular pathogen nutrient acquisition. Front Cell Infect Microbiol. 2015; 5:51.doi: 10.3389/fcimb.2015.00051 [PubMed: 26106587]
29. Escoll P, Roland M, Buchreiser C. Modulation of host autophagy during bacterial infection: Sabotaging host munitions for pathogen nutrition. Front Immunol. 2016; 7:81.doi: 10.3389/fimmu.2016.00081 [PubMed: 26973656]
30. Shih KM, Gerenday A, Fallon AM. Culture of mosquito cells in Eagle's medium. In Vitro Cell Develop Biol Anim. 1998; 34:629–630.
31. Oliva Chavez AS, Fairman JW, Felsheim RF, Nelson CM, Herron MJ, Higgins LA, et al. An 0-Methyltransferase Is required for Infection of tick cells by *Anaplasma phagocytophilum*. PloS Pathog. 2015; 11(11):e1005248.doi: 10.13/journal.ppat.1005248 [PubMed: 26544981]
32. Chen XG, Jiang X, Gu J, Xu M, Wu Y, Deng Y, et al. Genome sequence of the Asian tiger mosquito, *Aedes albopictus*, reveals insights into its biology, genetics, and evolution. Proc Nat Acad Sci USA. 2015; 112:5907–5915. DOI: 10.1073/pnas.1516410112.33
33. Keller A, Nesvizhskii A, Kolker E, Aebersold R. Empirical statistical model to estimate the accuracy of peptide identifications made by MS/MS and database seach. Anal Chem. 2002; 74:5383–5392. [PubMed: 12403597]
34. Nesvizhskii A, Keller A, Kolker E, Aebersold R. A statistical model for identifying proteins by tandem mass spectrometry. Anal Chem. 2003; 75:4646–4658. [PubMed: 14632076]
35. Shilov IM, Seymour SL, Patel AA, Loboda A, Tang WH, Kaeting SP, et al. The Paragon Algorithm, a next generation search engine that uses sequence temperature values and feature probabilities to identify peptides from tandem mass spectra. Mol Cell Proteomics. 2007; 6:1638–1655. [PubMed: 17533153]
36. Tang WH, Shilove IV, Seymour SL. Nonlinear fitting method for determining local false discovery rates from decoy database searches. J Proteome Res. 2008; 7:3661–3667. DOI: 10.1021/pr070492f [PubMed: 18700793]
37. Wright JD, Sjostrand FS, Portaro JK, Barr AR. The ultrastructure of the rickettsia-like microorganism *Wolbachia pipientis* and asssociated virus-like bodies in the mosquito *Culex pipiens*. J Ultrastructure Res. 1978; 63:79–85.
38. Wu M, Sun LV, Vamathevan J, Riegler M, Deboy R, Brownlie JC, et al. Phylogenomics of the reproductive parasite *Wolbachia pipientis w*Mel: a streamlined genome overrun by mobile gentic elements. PLoS Biol. 2004; 2doi: 10.1371/journal.pbio.002006939
39. Fafournoux P, Bruhat A, Jousse C. Amino acid regulation of gene expression. Biochem J. 2000; 351:1–12. [PubMed: 10998343]
40. Brasse-Lagnel C, Lavoinne A, Husson A. Control of mammalian gene expression by amino acids, especially glutamine. FEBS J. 2009; 276:1826–44. DOI: 10.1111/j.1742-4658.2009.06920.x [PubMed: 19250320]
41. Fallon AM, Witthuhn BA. Proteasome activity in a naïve mosquito cell line infected with *Wolbachia pipientis w*AlbB. In Vitro Cell Dev Biol Anim. 2009; 45:460–466. DOI: 10.1007/s11626-009-9193-6 [PubMed: 19296184]
42. Price CT, Al-Khodor S, Al-Quadan T, Santic M, Habyarimana F, Kalia A, et al. Molecular mimicry by an F-box effector of *Legionella pneumophila* hijacks a conserved polyubiquitin machinery within macrophages and protozoa. PLoS Pathog. 2009; 5:e1000704.doi: 10.1371/journal.ppat.1000704 [PubMed: 20041211]

43. Blitvich BJ, Firth A. Insect-specific flaviviruses: A systematic review of their discovery, host range, mode of transmission, superinfection exclusion potential and genomic organization. Viruses. 2015; 7:1927–1959. DOI: 10.3390/v7041927 [PubMed: 25866904]
44. O'Neill SL, Pettigrew M, Sinkins SP, Braig HR, Andreadis TG, Tesh RB. In vitro cultivation of *Wolbachia pipientis* in an *Aedes albopictus* cell line. Insect Mol Biol. 1997; 6:33–39. [PubMed: 9013253]
45. Dobson SL, Marsland EJ, Veneti Z, Bourtzis K, O'Neill SL. Characterization of *Wolbachia* host range via the in vitro establishment of infections. Applied Environ Microbiol. 2002; 68:656–660.
46. Fallon, AM. Transfection of cultured mosquito cells. In: Crampton, JM.Beard, CB., Louis, C., editors. The Molecular Biology of Insect Disease Vectors. Chapman and Hall; New York: 1997. p. 430-443.
47. Wright JD, Barr R. The ultrastructure and symbiotic relationships of *Wolbachia* of mosquitoes of the *Aedes scutellaris* group. J Ultrastructure Res. 1980; 72:52–64.
48. Fallon AM, Baldridge GB, Carroll EM, Kurtz CM. Depletion of host cell riboflavin reduces *Wolbachia* levels in cultured mosquito cells. In Vitro Cell Dev Biol Anim. 2014; 50:707–713. DOI: 10.1007/s11626-014-9758-x [PubMed: 24789726]
49. Fallon AM, Kurtz CM, Carroll EM. The oxidizing agent, paraquat, is more toxic to *Wolbachia* than to mosquito host cells. In Vitro Cell Dev Biol Anim. 2013; 49:501–507. DOI: 10.1007/s11626-013-9634-0 [PubMed: 23719839]
50. Sehrawat N, Gakhar SK. Mosquito proteomics: present and future perspectives. Res Biotechnol. 2014; 5:25–33. 2014.
51. Hortsch M, Goodman CS. Cell and substrate adhesion molecules in *Drosophila*. Annu Rev Cell Biol. 1991; 7:505–557. [PubMed: 1809354]
52. Fallon AM. Cytological properties of an *Aedes albopictus* mosquito cell line infected with *Wolbachia* strain *w*AlbB. In Vitro Cell Dev Biol-Anim. 2008; 44:154–161. DOI: 10.1007/s11626-008-9090-4 [PubMed: 18401667]
53. Barthalay Y, Hipeau-Jacquotte R, de la Escalera S, Jiminez F, Piovant M. *Drosophila* neurotactin mediates heterophilic cell adhesion. EMBO J. 1990; 9:3603–09. [PubMed: 2120048]
54. Fallon AM, Sun D. Exploration of mosquito immunity using cells in culture. Insect Biochem Mol Biol. 2001; 31:263–278. [PubMed: 11167096]
55. Hutchison CA, Chuang R-Y, Noskov VN, Assad-Garcia N, Deerinck TJ, Ellisman MH, et al. Design and synthesis of a minimal bacterial genome. Science. 2016(351):1414.
56. Beyenbach KW, Wieczorek H. The V-type H^+ ATPase: molecular structure and function, physiological roles and regulation. J Exp Biol. 2006; 209:577–589. [PubMed: 16449553]
57. Zoncu R, Bar-Peled L, Efeyan A, Wang S, Sancak Y, Sabatini DM. mTORC1 senses lysosomal amino acids through an inside-out mechanism that requires the vacuolar H^+-ATPase. Science. 2011; 334:678–683. DOI: 10.1126/science.1207056 [PubMed: 22053050]
58. Marchesini N, Vieira M, Luo S, Moreno SNJ, Docampo R. A malaria parasite-encoded Vacuolar H +-ATPase is targeted to the host erythrocyte. J Biol Chem. 2005; 280:36841–47. DOI: 10.1074/jbc.M507727200 [PubMed: 16135514]
59. Kang S, Shields AR, Jupatanakul N, Dimopoulos G. Suppressing Dengue-2 infection by chemical inhibition of *Aedes aegypti* host factors. PLoS Negl Trop Dis. 2014; 8:e3084.doi: 10.1371/journal.pntd.0003084 [PubMed: 25101828]
60. Sessions OM, Barrows NJ, Souza-Neto JA, Robinson TJ, Hershey CL, Rodgers MA, et al. Discovery of insect and human dengue virus host factors. Nature. 2009; 458:1047–1050. DOI: 10.1038/nature07967 [PubMed: 19396146]
61. Hao W, Chang CP, Tsao CC. Oligomycin-induced bioenergetic adaptation in cancer cells with heterogeneous bioenergetic organization. J Biol Chem. 2010; 285:12647–54. DOI: 10.1074/jbc.M109.084194 [PubMed: 20110356]
62. Meijer AJ, Lorin S, Blommaart EF, Codogno P. Regulation of autophagy by amino acids and MTOR-dependent signal transduction. Amino acids. 2015; 47:2037–63. DOI: 10.1007/s00726-014-1765-4 [PubMed: 24880909]

63. Foissner I, Sommer A, Hoeftberger M, Hoepflinger MC, Absolonova M. Is wortmannin-induced reorganization of the trans-Golgi network the key to explain charasome formation? Front Plant Sci. 2016; 7:756. doi:10.3389.fpls.2016.00756. [PubMed: 27375631]
64. Zois CE, Harris AL. Glycogen metabolism has a key role in the cancer microenvironment and provides new targets for cancer therapy. J Mol Med. 2016; 94:137–154. DOI: 10.1007/s00109-015-1377-9 [PubMed: 26882899]
65. Molloy JC, Sinkins SP. *Wolbachia* do not induce reactive oxygen species-dependent immune pathway activation in *Aedes albopictus*. Viruses. 2015; 7:4624–39. DOI: 10.3390/v7082836 [PubMed: 26287231]
66. Gerenday A, Fallon AM. Increased levels of the cell cycle inhibitor protein, dacapo, accompany 20-hydroxyecdysone-induced G1 arrest in a mosquito cell line. Arch Insect Biochem Physiol. 2011; 78:61–73. DOI: 10.1002/arch.20440.64 [PubMed: 21928393]
67. Huang Y-J, Higgs S, Horne KM, Vanlandingham DL. Flavivirus-mosquito interactions. Viruses. 2014; 6:4703–30. DOI: 10.3390/v6114703 [PubMed: 25421894]
68. Goddard LB, Roth AE, Reisen WK, Scott TW. Vertical transmission of West Nile virus by three California *Culex* (Diptera: Culicidae) species. J Med Entomol. 2003; 40:743–746. [PubMed: 14765647]
69. Mishra AC, Mourya DT. Transovarial transmission of West Nile virus in *Culex vishnui* mosquito. Indian J Med Res. 2001; 114:212–214. [PubMed: 12040765]
70. Stollar V, Thomas VL. An agent in the *Aedes aegypti* cell line (Peleg) which causes fusion of *Aedes albopictus* cells. Virology. 1975; 64:367–377. [PubMed: 806166]
71. Rainey SM, Shah P, Kohl A, Dietrich I. Understanding the *Wolbachia*-mediated inhibition of arboviruses in mosquitoes: progress and challenges. J Gen Virol. 2014; 95:517–530. DOI: 10.1099/vir.0.057422-0 [PubMed: 24343914]
72. Villar M, Ayllon N, Alberdi P, Moreno M, Tobes R, Mataeos-Hernandez L, et al. Integrated metabolomics, transcriptomics and proteomics identifies metabolic pathways affected by *Anaplasma phagocytophilum* infection in tick cells. Mol Cell Proteomics. 2015; 14:3154–72. DOI: 10.107/mcp.M115.051938 [PubMed: 26424601]

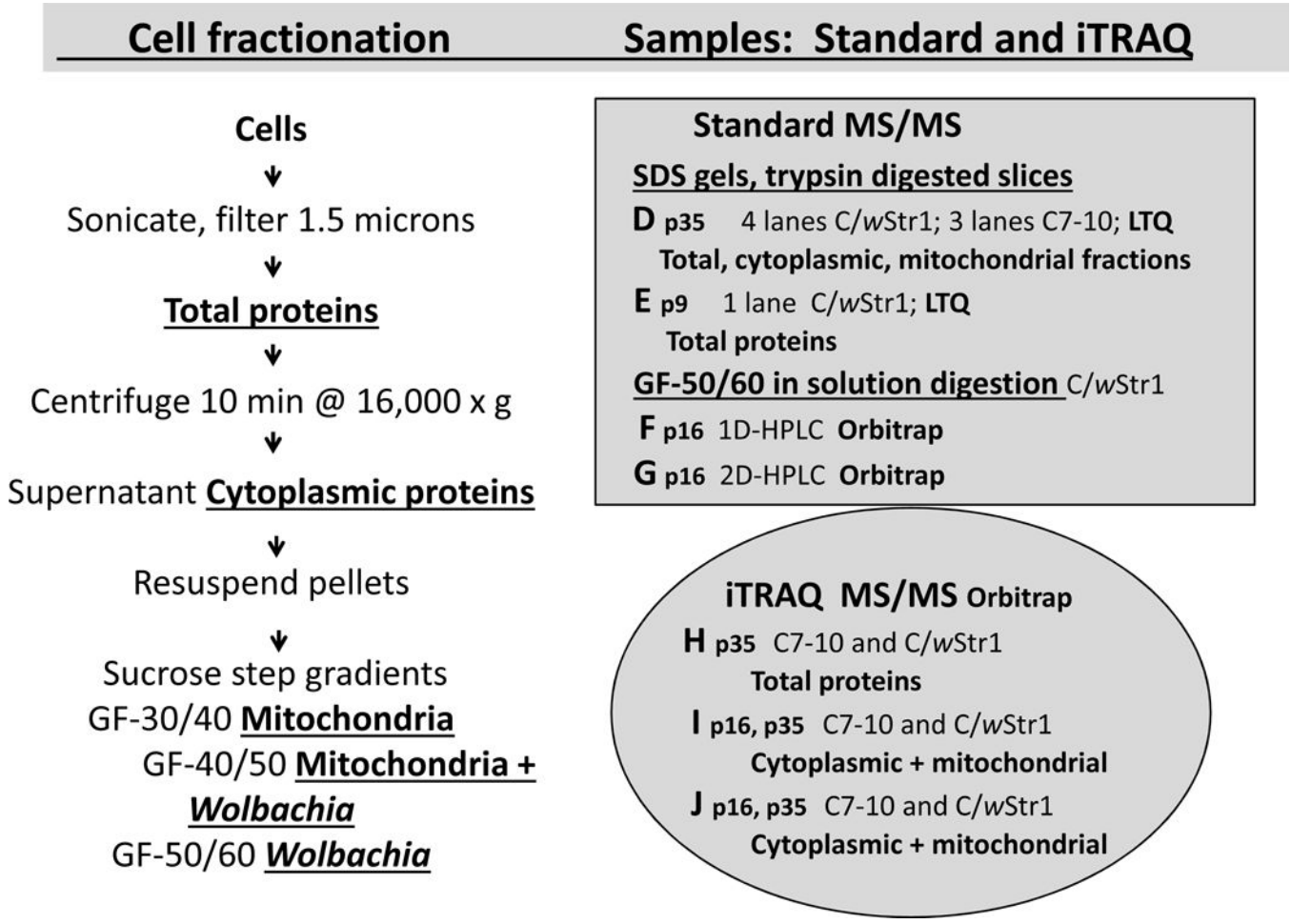

Fig. 1.

Sample preparation for MS/MS analysis. Samples were prepared according to the flow chart at left as detailed earlier by Baldridge et al. [27]. Underlined, bold text designates fractions used in the analyses at right. The shaded rectangle shows samples D (p16), E (p9), F (p16) and G (p16), from which host proteins were identified in a standard analysis, and the shaded oval represents samples H (p35), I, (p16 and p35) and J (p16 and p35) used for iTRAQ analysis; note that "p" designates passage number. Samples for MS data sets D and E were separated by SDS-PAGE and recovered from gel slices that were trypsin-digested in situ for protein identification by LTQ MS/MS. Data sets F and G were derived from the *Wolbachia*-enriched gradient fraction GF-50/60 digested in-solution with trypsin for HPLC separation of peptides and protein identification by Orbitrap MS/MS [27]. For the iTRAQ analysis, aliquots of total, cytoplasmic or mitochondrial fractions (pooled GF-30/40 and GF-40/50) from C7–10 and C/*w*Str1 cells were labeled with isobaric tags in three 4-plex reactions for protein identification by Orbitrap MS/MS.

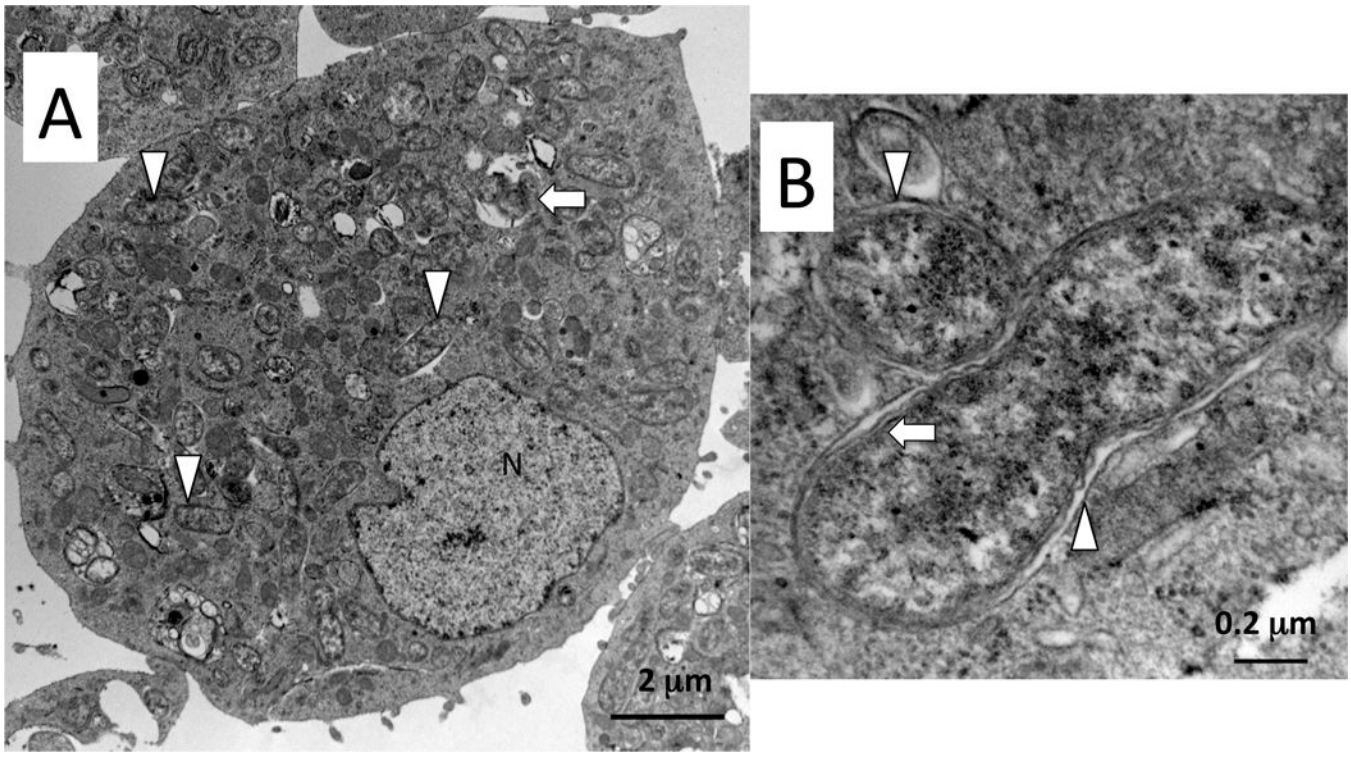

Fig. 2.

Representative transmission electron micrographs of C/*w*Str1 cells at near confluency. A) Host cell containing coccoid and elongate (arrowheads) *w*Str whose profiles range from ≈ 0.4–1.1 microns. Some inclusions appear to contain *Wolbachia* undergoing degradation (arrow). N, nucleus. B) *Wolbachia* in vertical and horizontal cross-section. Note the separation between the host-derived vacuolar membrane (arrowheads) and the bacterial cell wall, electron-lucent periplasmic space and inner periplasmic membrane (arrow).

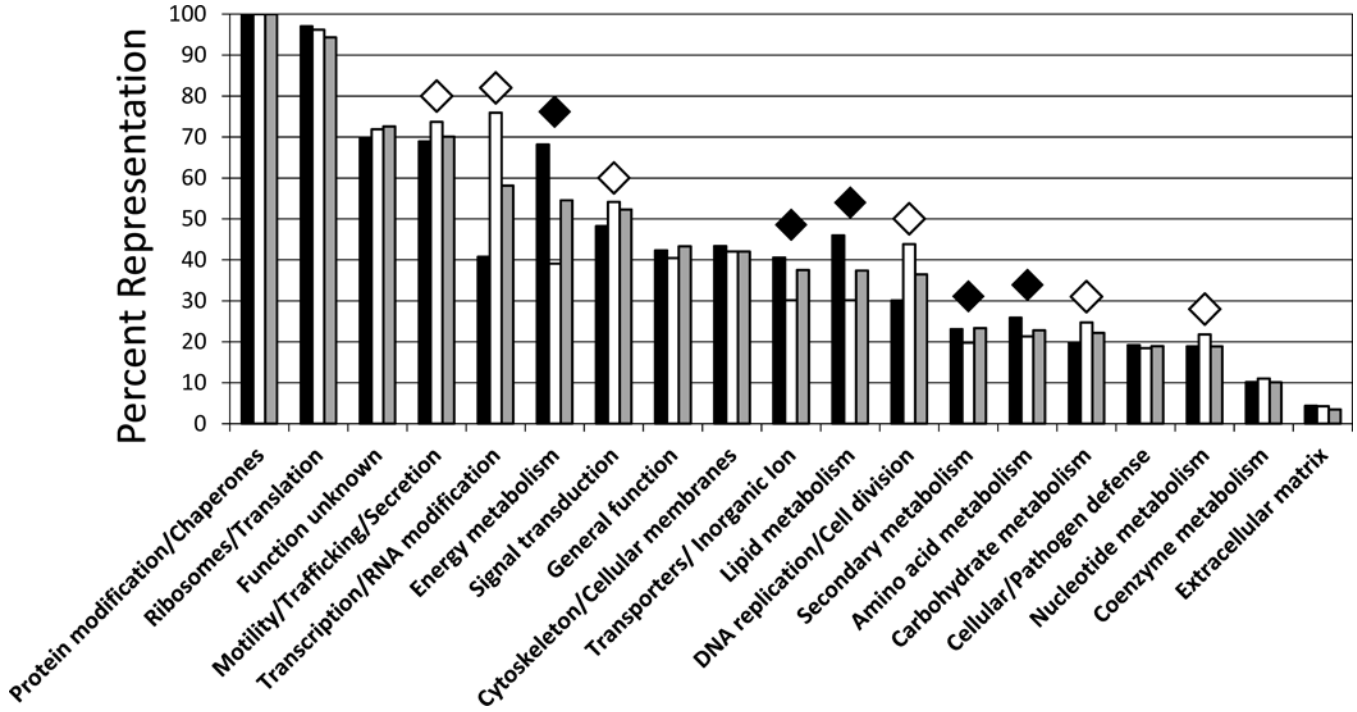

Fig. 3.

Distribution of identified *Aedes* host proteins by functional class. Individual protein identifications (8,313) in standard data sets D and E (see Table 1 and Fig. 1) and iTRAQ data sets H, I and J (3,177 identifications) were grouped into functional classes and normalized to numbers in the largest class, Protein modification/chaperones, defined as 100%. Functional classes were sorted left to right based on decreasing percentages in iTRAQ (gray bars). Diamond symbols indicate functional classes in which the ratio of C/*w*Str1 (black bars) relative to C7–10 (white bars) ranged from 0.5–0.9 (white diamonds) or 1.2–1.7 (black diamonds). Note that over 30% of proteins in the small Inorganic ion metabolism class (Table S1, sheet 1) have roles in ion transport and have been merged with the larger transporters class.

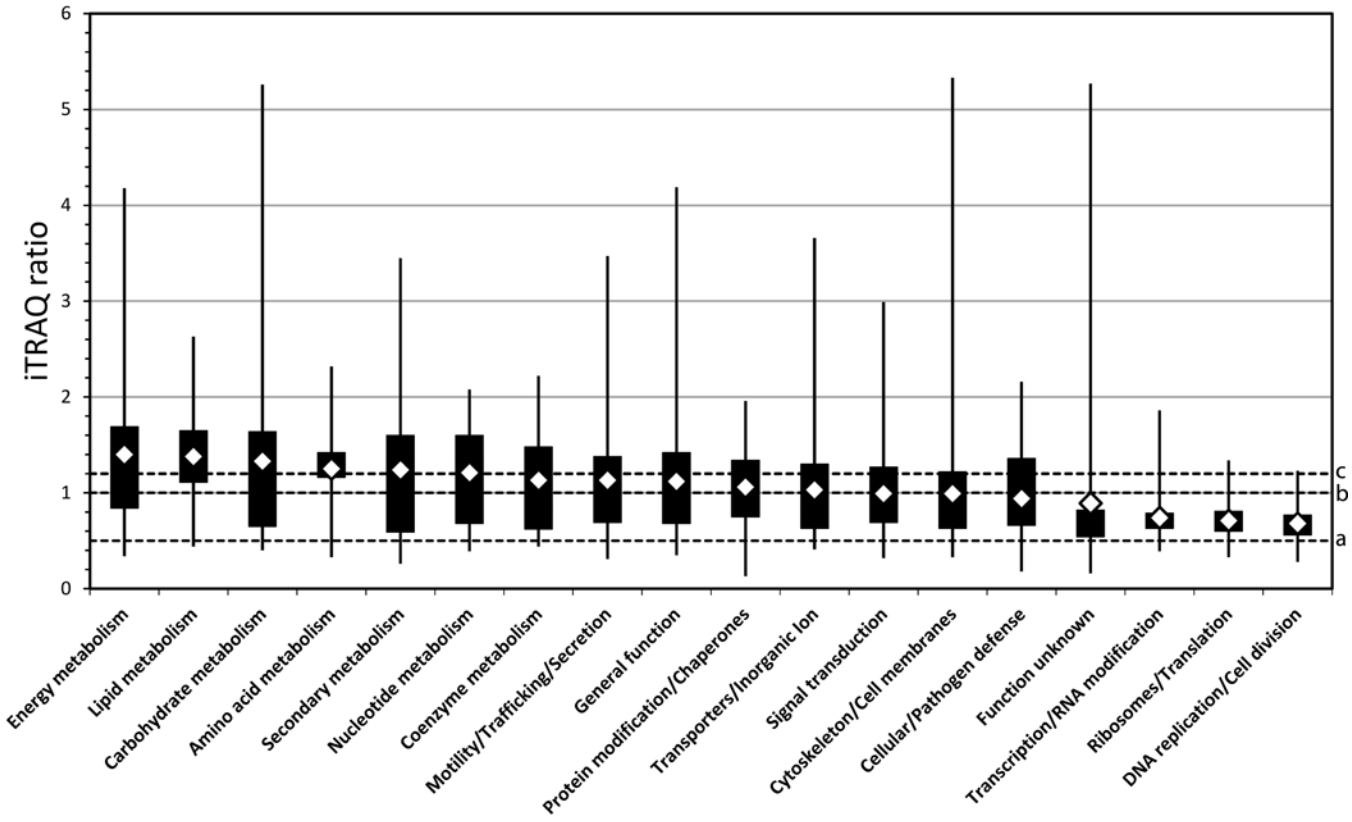

Fig. 4.

Distribution of *Aedes* host proteins with differential iTRAQ ratios by functional class. Average ratios by functional class were calculated from 1,307 observations (representing 815 consensus proteins listed in Table S4). Ratios are depicted in decreasing order on a linear scale, which was converted to log scale for statistical analyses described in the text. Diamonds indicate mean ratios (listed in Table 4), filled boxes represent first through third quartiles, and bars indicate minimum and maximum values. A small number of proteins with differential ratios in the inorganic ion and extracellular matrix class were included in the transporter and cytoskeleton/cell membrane classes, respectively.

Table 1

Cumulative *Aedes albopictus* and *Wolbachia* strain *w*Str protein identifications.

	***Aedes albopictus* proteins**				***Wolbachia w*Str proteins**			
Data set[a]	**Total Cell[b]**	**Cyto.[c] Mito[d]**	**Wolb.[e] enrich**	**Total *Aedes*[f]**	**Tot. Cell[b]**	**Cyto[c] Mito[d]**	**Wolb.[e] enrich**	**Total *w*Str[f]**
D (gel, C7–10)	1373	2271	–	3644	–	–	–	–
D (gel, C/*w*Str1)	1199	1791	859	3849	*391*	*746*	*521*	*1658*
E (gel, C/*w*Str1)	820	–	–	820	*404*	–	–	*404*
F, G (C/*w*Str1)	–	–	1535	1535	–	–	*851*	*851*
All data sets	3392	4062	2394	9848	*795*	*746*	*1372*	*2913*
Consensus				1859				*790*
H (iTRAQ)	1616			1616		110		110
I (iTRAQ)	–	968	–	968	241	284	–	525
J (iTRAQ)	–	593	–	593	–	–	–	–
All data sets	1616	1561	–	3177	241	394	–	635
Consensus				2016				327
Aggregate total				2471				790

[a] See Figure 1 for protein extracts included in each data set.

[b] Total cellular proteins.

[c] Cytoplasmic subcellular fraction proteins.

[d] Mitochondrial subcellular fraction proteins.

[e] Wolbachia-enriched subcellular fraction proteins.

[f] All fractions combined. Total values for data sets D–G and H–J, respectively indicate the aggregate number of identifications from all cellular fractions. Consensus values indicate the total number of unique proteins identified from all data sets. Aggregate total indicates number of consensus proteins from combined Standard and iTRAQ data sets. Note that iTRAQ protein identifications were derived from equal mass mixtures of C/*w*Str1 and C7–10 protein extracts. Values in italic font were previously described in detail [27].

Table 2

Statistical summary of *Aedes* proteins with differential iTRAQ ratios in C/*w*Str1 relative to C7–10 cells.

Protein functional class	# Proteins	% Total	N[a]	Mean[b]	Beta[c]
Lipid metabolism	39	4.79	61	0.23 (0.44)	0.54716
Energy metabolism	61	7.48	116	0.22 (0.52)	0.53115
Amino acid metabolism	26	3.19	45	0.14 (0.45)	0.45108
Carbohydrate metabolism	25	3.07	49	0.11 (0.61)	0.42181
Nucleotide metabolism	21	2.58	35	0.09 (0.50)	0.40186
Secondary metabolism	25	3.07	41	0.01 (0.67)	0.32779
Coenzyme metabolism	14	1.72	19	0.01 (0.50)	0.31945
Motility/Trafficking/Secretion	59	7.24	96	–0.02 (0.52)	0.28941
Protein modification/Chaperones	87	10.67	139	–0.03 (0.45)	0.28605
General function	45	5.52	61	–0.04 (0.52)	0.27744
Transporters/Inorganic ion metabolism[e]	34	4.17	48	–0.08 (0.47)	0.23015
Signal transduction	39	4.79	52	–0.12 (0.45)	0.19667
Cytoskeleton/Cellular membranes[f]	51	6.26	91	−0.14 (0.47)	0.17712
Cellular/Pathogen defense	22	2.70	34	−0.21 (0.59)	0.10285
Transcription/RNA modification	52	6.38	76	−0.34 (0.27)	−0.02330
Ribosomes/Translation	110	13.50	192	−0.37 (0.23)	−0.05360
DNA replication/Cell division	44	5.40	69	−0.42 (0.27)	−0.10658
Function unknown[d]	61	7.48	83	−0.31 (0.56)	0 (referent)[d]

[a]Number of differential iTRAQ ratios from MS data sets H, I and J; Total of 1307 ratios representing 815 proteins (Table S3, sheet 1).

[b]Mean (standard deviation) of log transformed iTRAQ ratios in C/*w*Str1 relative to C7–10 extracts.

[c]Beta coefficient of functional class in univariable linear regression model; mean of all classes excluding function unknown is 0.24314.

[d]Function unknown was modeled as the referent class.

[e]Transporter and Inorganic ion metabolism functional classes merged.

[f]Cytoskeleton/Cellular membrane and Extracellular matrix functional classes merged.

Res Microbiol. Author manuscript; available in PMC 2018 September 01.

Table 3

Summary of iTRAQ protein ratios from Table S4.

Protein functional class[a]	Sheet[b]	Total (%)[c]	Ave.[d]	Range[e]	> 1.2 (%)[f]	≥ 2 (%)[g]
Energy metabolism	1	61 (7.5%)	1.24 (1.40)	0.35–2.65	35 (57%)	5 (8%)
Lipid metab.	2	39 (4.8%)	1.42 (1.38)	0.48–2.63	29 (74%)	4 (10%)
Carbohydrate metab.	3	25 (3.1%)	1.24 (1.33)	0.42–3.06	16 (64%)	2 (8%)
Amino acid metab.	4	26 (3.2%)	1.20 (1.25)	0.33–1.79	17 (65%)	0
Secondary metab.	5	25 (3.1%)	1.24 (1.24)	0.36–2.91	13 (52%)	4 (16%)
Nucleotide metab.	6	21 (2.6%)	1.22 (1.21)	0.46–2.07	13 (62%)	2 (10%)
Coenzyme metab.	7	14 (1.7%)	1.11 (1.13)	0.44–2.09	7 (50%)	1 (7%)
Motility/Trafficking/Secretion	8	59 (7.2%)	1.10 (1.13)	0.47–3.23	21 (36%)	6 (10%)
General function	9	45 (5.5%)	1.10 (1.12)	0.52–4.19	16 (36)	3 (7%)
Protein modifn/Chaperones	10	87 (10.7%)	1.06 (1.06)	0.27–1.85	38 (44%)	0
Transporters/Ions	11	34 (4.2%)	1.11 (1.03)	0.42–3.66	14 (41%)	1 (3%)
Signal transduction	12	39 (4.8%)	1.02 (0.99)	0.35–2.99	14 (36%)	2 (5%)
Cytoskeleton/Cell. membranes	13	51 (6.2%)	1.00 (0.99)	0.40–5.33	13 (25%)	2 (4%)
Cellular/Pathogen defense	14	22 (2.7%)	1.01 (0.94)	0.18–2.10	9 (41%)	1 (4%)
Function unknown	15	61 (7.5%)	0.88 (0.89)	0.29–5.01	12 (20%)	4 (7%)
Transcription/RNA modifn.	16	52 (6.4%)	0.73 (0.74)	0.49–1.79	1 (2%)	0
Ribosomes/Translation	17	110 (13.5%)	0.72 (0.71)	0.33–1.34	3 (3%)	0
DNA replication/Cell division	18	44 (5.4%)	0.69 (0.68)	0.45–1.18	0	0
Aggregate total		815 (100%)			271 (33%)	37 (4.5%)

[a] Protein functional class from Table S4.

[b] Sheet numbers in Table S4.

[c] Total number of proteins, with percentages.

[d] Arithmetic average of protein ratios (C/*w*Str1 over C7–10) with equal weight given to each of 815 proteins. (see Table S4). Weighted averages based on 1307 observations (see Fig. 4) are given in parentheses.

[e] Range of protein ratios.

[f] Number of proteins with ratios > 1.2, with percentages.

[g] Number of proteins with ratios > 2.0, with percentages.

Table 4

Top-37 *Aedes* iTRAQ proteins.

Identified proteins	Accession[a]	Ratio[b]	Functional class[c]
neurotactin	gi|157121167	5.33	Cytoskeleton/Cellular membranes
hypothetical protein AAEL001471	gi|157119483	5.01	Function unknown
apoptosis protein	gi|157124948	4.19	General function
hypothetical protein AAEL010818	gi|157127471	3.66	Transporters/Inorganic Ion metabolism
V-ATPase V_0 116 kDa subunit i	gi|157138700	3.23	Motility/Trafficking/Secretion
glycogen phosphorylase	gi|157108521	3.06	Carbohydrate metabolism
hypothetical protein AAEL010678	gi|157126928	2.99	Signal transduction
cytochrome P450	gi|157105117	2.91	Secondary metabolism
V-ATPase V_1 subunit C	gi|157109023	2.81	Motility/Trafficking/Secretion
V-ATPase V_1 subunit H	gi|157113604	2.75	Motility/Trafficking/Secretion
V-ATPase V_1 subunit D	gi|157124332	2.73	Motility/Trafficking/Secretion
malate dehydrogenase	gi|157116681	2.65	Energy metabolism
3-hydroxyl-coa dehydrogenase	gi|157132312	2.63	Lipid metabolism
hypothetical protein AAEL013851	gi|157137775	2.61	General function
3-hydroxyl-coa dehydrogenase	gi|157117489	2.52	Lipid metabolism
CRAL/TRIO domain-containing protein	gi|157135818	2.50	General unknown
cytochrome p450	gi|157167202	2.50	Secondary metabolism
phophoenolpyruvate carboxykinase	gi|157103343	2.48	Energy metabolism
cytochrome c oxidase subunit iv	gi|157108935	2.43	Energy metabolism
lethal(2)essential for life protein, l2efl	gi|157135547	2.39	Function unknown
citrate synthase	gi|157133341	2.24	Energy metabolism
hypothetical protein AAEL002350	gi|157128286	2.22	Function unknown
V-ATPase subunit E	gi|157131212	2.20	Motility/Trafficking/Secretion
hypothetical protein AAEL002861	gi|157132592	2.17	Function unknown
choline-phosphate cytidylyltransferase a, b	gi|157129766	2.12	Lipid metabolism
phosphorylase kinase, gamma, partial	gi|157137241	2.12	Signal transduction
glutathione peroxidase	gi|157118772	2.10	Cellular/Pathogen defense
beta-alanine synthase, putative	gi|157112908	2.09	Coenzyme metabolism
zeta coat protein	gi|157134570	2.08	Motility/Trafficking/Secretion
adenosine diphosphatase	gi|157110697	2.07	Nucleotide metabolism
annexin B9	gi|157129014	2.05	Cytoskeleton/Cellular membranes
aldehyde dehydrogenase, putative	gi|157131682	2.05	Secondary metabolism
phosphofructokinase	gi|157114499	2.04	Energy metabolism
short chain type dehydrogenase	gi|157107865	2.04	Lipid metabolism
adenylate kinase 3, putative	gi|157106105	2.02	Nucleotide metabolism
estradiol 17 beta-dehydrogenase	gi|157114880	2.02	Secondary metabolism
phophoglucomutase	gi|157124898	2.00	Carbohydrate metabolism

[a]Host proteins with iTRAQ ratios ≥ 2.00 from Table S4. V-ATPase subunits are shaded dark gray, and hypothetical proteins are shaded light gray.

[b] NCBI accession number.

[c] iTRAQ ratio (C/*w*Str1 over C7–10).

[d] Protein functional class.

Res Microbiol. Author manuscript; available in PMC 2018 September 01.

Table 5

Aedes hypothetical proteins with high and low iTRAQ ratios.

Hypothetical proteins[a]	Accession[b]	kDa[c]	Ratio (avg)[d]	Functional class[e]	Comments/pathways
AAEL001471	gi|157119483	82	5.01	Function unknown	Zinc finger, ubiquitin-binding, signaling
AAEL010818	gi|157127471	22	3.66	Transporters/Inorganic Ion	homology to mitochondrial phosphate carrier protein
AAEL010678	gi|157126928	44	2.99	Signal transduction	phospholipase C-like phosphodiesterases domain
AAEL013851	gi|157137775	27	2.61	General function	modifies proteins associated with ribosomes, translation
AAEL002350	gi|157128286	18	2.22	Function unknown	DU1075 domain of unknown function
AAEL002861	gi|157132592	48	2.17	Function unknown	saccharopine dehydrogenase; lysine metabolism in fungi
AAEL003651	gi|157137711	57	1.86	Lipid metabolism	phopholipases associated with Golgi membranes
AAEL010116	gi|157125198	60	1.69	Transporters/Inorganic Ion	mitochondrial Calcium uptake protein; calcium sensor
AAEL008454	gi|157118896	23	1.61	Secondary metabolism	catalyses isochorismate to 2,3-dihydroxybenzoate and pyruvate
AAEL012863	gi|157133791	27	1.61	General function	probable member RIM1 Acetyltransferases COG0456
AAEL008862	gi|157119998	113	1.56	General function	probable zinc-dependent peptidase
AAEL006343	gi|157113179	69	1.55	Function unknown	VCBS repeat domain; immunomodulatory protein
AAEL007236	gi|157115555	32	0.5	Secondary metabolism	Farnesoic acid O-methyl transferase.
AAEL014011	gi|157138509	93	0.49	Function unknown	ankyrin domain
AAEL002691	gi|157131093	143	0.48	Function unknown	SMC domain for chromosome maintenance
AAEL006364	gi|157113255	43	0.48	Carbohydrate metabolism	Amino sugar and nucleotide sugar metabolism
AAEL014194	gi|157103922	27	0.46	Function unknown	similarity to Microtubule-associated
AAEL004180	gi|157104866	51	0.44	Coenzyme metabolism	probable ubiquinone monooxygenase
AAEL004958	gi|157108115	62	0.43	Secondary metabolism	Farnesoic acid O-methyl transferase domain
AAEL002115	gi|157126696	56	0.42	Function unknown	Zinc finger domain
AAEL005141	gi|157108846	26	0.4	Function unknown	signal peptide membrane domain
AAEL011155	gi|157128487	44	0.4	Function unknown	has DUF155 domain found in some yeast cyclins
AAEL014816	gi|157107145	54	0.39	Function unknown	70% similar to acidic membrane protein
AAEL008569	gi|157119197	25	0.35	Signal transduction	signal transduction protein; cyclin-dependent kinase cdk5
AAEL008658	gi|157119386	82	0.29	Function unknown	similar to UPF0183 proteins of unknown function

[a] NCBI protein definition; proteins from Table S4 with ratios > 1.5 shaded gray.

[b] NCBI protein accession number.

[c] Calculated molecular mass in kilodaltons.

[d] iTRAQ protein ratio (C/*w*Str1 over C7–10).

[e] Protein functional class.

Table 6

MS/MS peptides in C7–10 and C/*w*Str1 extracts matched to selected *Flavivirus* polyprotein sequences.

Flavivirus	Accession[a]	Peptides[b]	Coverage[c]	Vectors[d]	Hosts[e]
DENV4; Dengue	GI: 119390884	16	7.2	*Ae. aegypti* *Ae. albopictus*	primates
YFV; Yellow fever	GI: 383464646	15	6.7	*Ae. aegypti* *Hemagogus* spp.	primates
ZIK; Zika	GI: 146411781	11	5.3	*Ae. aegypti* *Ae. albopictus*	primates
JEV; Japanese encephalitis	GI: 12964701	27	13.5	*Aedes* spp. *Culex* spp. *Anopheles* spp.	mammals birds
WNV; West Nile virus	GI: 90025136	34	15.4	*Aedes* spp. *Culex* spp.	mammals birds
POW; Powassan virus	GI: 730353	7	3.6	*Aedes* spp. *Culex* spp.	mammals birds
TBEV; Tick-borne encephalitis	GI: 1066075	16	6.9	*Ixodes* ticks *Dermacentor* ticks	mammals
AeFV; Aedes Flavivirus	GI: 251823440	11	4.9	*Ae. aegypti* *Ae. flavopictus* *Culex pipiens*	mosquitoes
CxFV; Culex flavivirus	GI: 247893527	6	3.0	*Culex pipiens* *Culex tarsalis* *Culex nigripalpus* *Culex* spp.	mosquitoes
CFA; Cell fusion agent	GI: 464429	3	1.6	*Ae. aegypti* *Ae. albopictus* *Culex* spp.	mosquitoes

[a] Genbank accession numbers for polyprotein sequences, which undergo post-translational cleavage to produce three structural and seven nonstructural proteins (see Fig. S2).

[b] Total number of 95% confidence unique peptides.

[c] Percent polyprotein sequence coverage.

[d] Includes major arthropod vectors.

[e] Principal vertebrate hosts.